Journal of Neurochemistry

JOURNAL OF NEUROCHEMISTRY | 2009 | 110 | 1070–1081 doi: 10.1111/j.1471-4159.2009.06203.x

Tobacco carcinogen induces microglial activation and subsequent neuronal damage

Debapriya Ghosh, Manoj Kumar Mishra, Sulagna Das, Deepak Kumar Kaushik and Anirban Basu

National Brain Research Centre, Manesar, Haryana, India

Abstract

4-Methylnitrosamino-1-(3-pyridyl)-1-butanone (NNK) is a tobacco-specific procarcinogen. We have investigated whether NNK causes inflammatory upheaval in the brain by activation of resident microglia and astrocyte and result in bystander neuronal damage. We have carried out the work in both *in vitro* and *in vivo* models. We have found that treatment with NNK causes significant activation of mouse microglial (BV2) cell line as evident by increase in reactive oxygen species and nitric oxide level. Western blot analysis has showed increase in proinflammatory signaling proteins, proinflammatory effector proteins, and other stress-related proteins. Interestingly, increased levels of proinflammatory cytokines like interleukin (IL)-6, tumor necrosis factor-α, monocyte chemoattractant protein 1 (MCP1), and IL-12p70 are also detected. Work from our *in vivo* studies has demonstrated similar increase in proinflammatory signaling and effector molecules along with the proinflammatory cytokine levels, following NNK treatment. Immunohistochemical staining of the brain sections of NNK-treated mice reveals massive microglial and astrocyte activation along with distinct foci of neuronal damage. Both *in vitro* and *in vivo* results provide strong indication that NNK causes significant upheaval of the inflammatory condition of brain and inflicts subsequent neuronal damage.

Keywords: astrocytes, cytochrome P450, inflammation, microglia, neuron, tobacco carcinogen.

J. Neurochem. (2009) **110**, 1070–1081.

Several compounds of the cigarette smoke have been identified to have carcinogenic potency (Nakayama *et al.* 1985; Hecht *et al.* 1999). 4-*N*-methyl-*N*-nitrosamino-1-(3-pyridyl)-1-butanone (NNK), a major nitrosamine formed in tobacco smoke, is a very potent carcinogen (Jin *et al.* 2004). Concentrations of NNK in tobacco substances may vary widely (Akopyan and Bonavida 2006), (http://www.springerlink.com/content/j8l15k7025052204/). Both direct and second-hand tobacco smoke exposures lead to substantial measures of NNK intake.

One of the most important aspects of diseases that have been studied in the recent years is inflammation. Inflammation plays a pivotal role in extremely wide array of disease conditions ranging from viral diseases of CNS (Ghoshal *et al.* 2007) to neurodegenerative disorders (Griffin 2006). Few studies provide insights on the effect of tobacco smoke and inflammation (Hellermann *et al.* 2002; Weng *et al.* 2004). Although NNK has been reported to induce oxidative stress in the microsomal fraction of brain (Bhagwat *et al.* 1998), little work has been carried out to elucidate whether NNK can trigger neuroinflammation in brain and whether the inflamed milieu can cause any neuronal damage. Considering the extreme economical and disease burden of the neuroinflammation-related disorders (http://www.ingentaconnect.com/content/ftd/erp/2006/00000006/00000002/art00007) (Menzin *et al.* 1999), it is extremely important from medical, social, and economic point of view to elucidate whether NNK could cause neuroinflammation.

Our present study conducted in both *in vitro* and *in vivo* model systems showed that NNK could cause robust

Received April 3, 2009; revised manuscript received May 20, 2009; accepted May 27, 2009.

Address correspondence and reprint requests to Anirban Basu, National Brain Research Centre, Manesar, Haryana 122050, India. E-mail: anirban@nbrc.ac.in

Abbreviations used: CBA, cytokine bead array; COX-2, cyclooxygenase 2; ERK1/2, extracellular regulated kinase; FJC, Flouro Jade C; GFAP, glial fibrillary acidic protein; HSP, heat shock protein; IL, interleukin; iNOS, induced inducible nitric oxide; JNK, c-*Jun* N-terminal kinase; MAPK, mitogen-activated protein kinase; MCP1, monocyte chemoattractant protein 1; MTT, 3-(4,5-dimethylthiazol-2-yl)-2,5-diphenyltetrazolium bromide; NF, nuclear factor; NNK, 4-*N*-methyl-*N*-nitrosamino-1-(3-pyridyl)-1-butanone; NO, nitric oxide; PBS, phosphate-buffered saline; ROS, reactive oxygen species; SOD, superoxide dismutase; TNF, tumor necrosis factor; TRX1, thioredoxin 1.

microglial activation leading to profound increase in inflammatory mediators. Our study extended further to show that the inflamed milieu may cause neuronal damage.

Materials and methods

Cell lines and animals

Detailed information of cell lines and animals used are provided in the Appendix S1. Mouse neuroblastoma cell line (N2a), microglial cell line (BV2), and cortical neurons were used for *in vitro* studies. Cortical neurons were obtained following a published protocol (Gao *et al.* 1991) but with substantial modification. Adult BALB/c mice (6 weeks) of either sex were used in all *in vivo* experiments.

MTT assay

Mouse neuroblastoma Neuro2a cells (N2a) and mouse microglial cells (BV2) were plated in 96-well plate at a density of 2×10^4 cells/well and were cultured for 24 h in 200 μL of Dulbecco's modified Eagle's medium (Sigma, St Louis, MO, USA) with 10% fetal bovine serum (Sigma). After 24 h, the cells were switched to serum-free media for additional 12 h. Cells were then treated with various concentrations of NNK for 48 h. The viability was then evaluated by 3-(4,5-dimethylthiazol-2-yl)-2,5-diphenyltetrazolium bromide (MTT; Sigma) assay as described elsewhere (Swarup *et al.* 2008).

3-(4,5-Dimethylthiazol-2-yl)-2,5-diphenyltetrazolium bromide assay was also performed on the primary cortical neurons plated in the 96-well plates after treating the cells with various concentrations of NNK for 48 h. The primary neuronal cells plated in Labtek chamber slide (Labtek, Roskilde, Denmark) were fixed in 4% paraformaldehyde for 20 min, and then stained for Beta III Tubulin (Promega Corporation, Madison, WI, USA). The slides were observed under Zeiss Axioplan 2 Fluorescence microscope (Zeiss, Gottingen, Germany).

Measurement of reactive oxygen and nitrogen species

BV2 cells were plated in low density and allowed to grow for 24 h in Dulbecco's modified Eagle's medium with 10% fetal bovine serum. Cells were then switched to serum-free media for 12 h and then treated with 500 μM of NNK for various time points. The level of reactive oxygen species (ROS) produced within cells was then monitored fluorimetrically by Varioskan Flash Multimode Reader (Thermo Electron Corporation, Vantaa, Finland) using the dye 5-and 6-chlromethyl-20,70-dichlorodihydrofluorescein diacetate (Sigma) according to a process previously described (Mishra *et al.* 2007). Reactive nitrogen species and nitric oxide (NO) levels in cell supernatant was measured by Griess reagent as previously described (Mookerjee Basu *et al.* 2006).

Immunoblot

Immunoblot analysis was performed against cyclooxygenase 2 (COX-2), induced inducible nitric oxide (iNOS), phospho-extracellular regulated kinase (ERK1/2), phospho-p38 mitogen-activated protein kinase (MAPK), phospho-c-*Jun* N-terminal kinase (JNK), phospho-nuclear factor (NF)κβ, NFκβ, IκBα heat shock protein (HSP70), superoxide dismutase (SOD)-1, and thioredoxin 1 (TRX1) using respective antibodies at 1 : 1000 dilutions. Details of the immunoblot procedure are provided in the Appendix S1.

Cytokine bead array

The BD mouse cytokine bead array (CBA) kits (mouse inflammation CBA kit; BD Biosciences, San Diego, NJ, USA) were used to quantitatively measure cytokine levels in BV2 cell lysates and mouse whole-brain lysates. Fifty μL of mouse inflammation standard and sample dilutions were used and the assay was performed according to the manufacturer's instructions and analyzed on the FACS Calibur (BD Biosciences) (Swarup *et al.* 2007).

Immunohistochemsitry

Animals from control and treated groups of both 4 and 12 days experiments were perfused and the brains were processed for cryostat sectioning (Basu *et al.* 2002; Ghoshal *et al.* 2007). To label activated microglia, activated astrocytes and neurons, sections were incubated overnight at 4°C with rabbit anti-Iba-1 (Wako, Osaka, Japan), rabbit anti-glial fibrillary acidic protein (GFAP) (Dako, Glostrup, Denmark), and mouse anti-NeuN (Chemicon, Concord Road, MA, USA) respectively at dilutions of 1 : 500. After washes, slides were incubated with appropriate secondary antibodies conjugated with fluorescein (Vector Laboratories, Burlingame, CA, USA) and following final washes, sections were mounted. All the slides were observed under Zeiss Axioplan 2 Fluorescence microscope or Zeiss Confocal microscope (Zeiss).

Histochemistry

Cryostat sections were also processed for thionin (Basu *et al.* 2005) and Flouro Jade C (FJC; Chemicon) staining (Schmued *et al.* 2005). The thionin-stained sections were then observed under Leica 4000 DB light microscope (Leica Microsystems, Wetzlar, Germany). FJC-stained slides were observed under Zeiss Axioplan 2 Fluorescence microscope (Zeiss).

Statistical analysis

The data generated from the experiments were analyzed statistically using One-way model 1 ANOVA followed by Holm–Sidak multiple comparision test using SigmaStat 3.5 (Sigma, Chicago, IL, USA). A level of $p < 0.05$ was considered significant.

Results

NNK does not cause direct neuronal or microglial cytotoxicity *in vitro*

Previous experiments with human bronchiolar and alveolar cell lines (BEAS2B and A549, respectively) treated with 500 μM NNK, showed substantial immunomodulatory effect of NNK on these cell lines (Proulx *et al.* 2005). Thus, we wanted to know the effect of 500 μM NNK on N2a and BV2 cell lines. To assess the direct cytotoxicity that NNK might be having on the neuronal and microglial cell line, we performed the MTT assay after treating N2a cells and BV2 cells plated in 96-well plate with various concentrations of NNK for 48 h. Results of the MTT assay showed that NNK

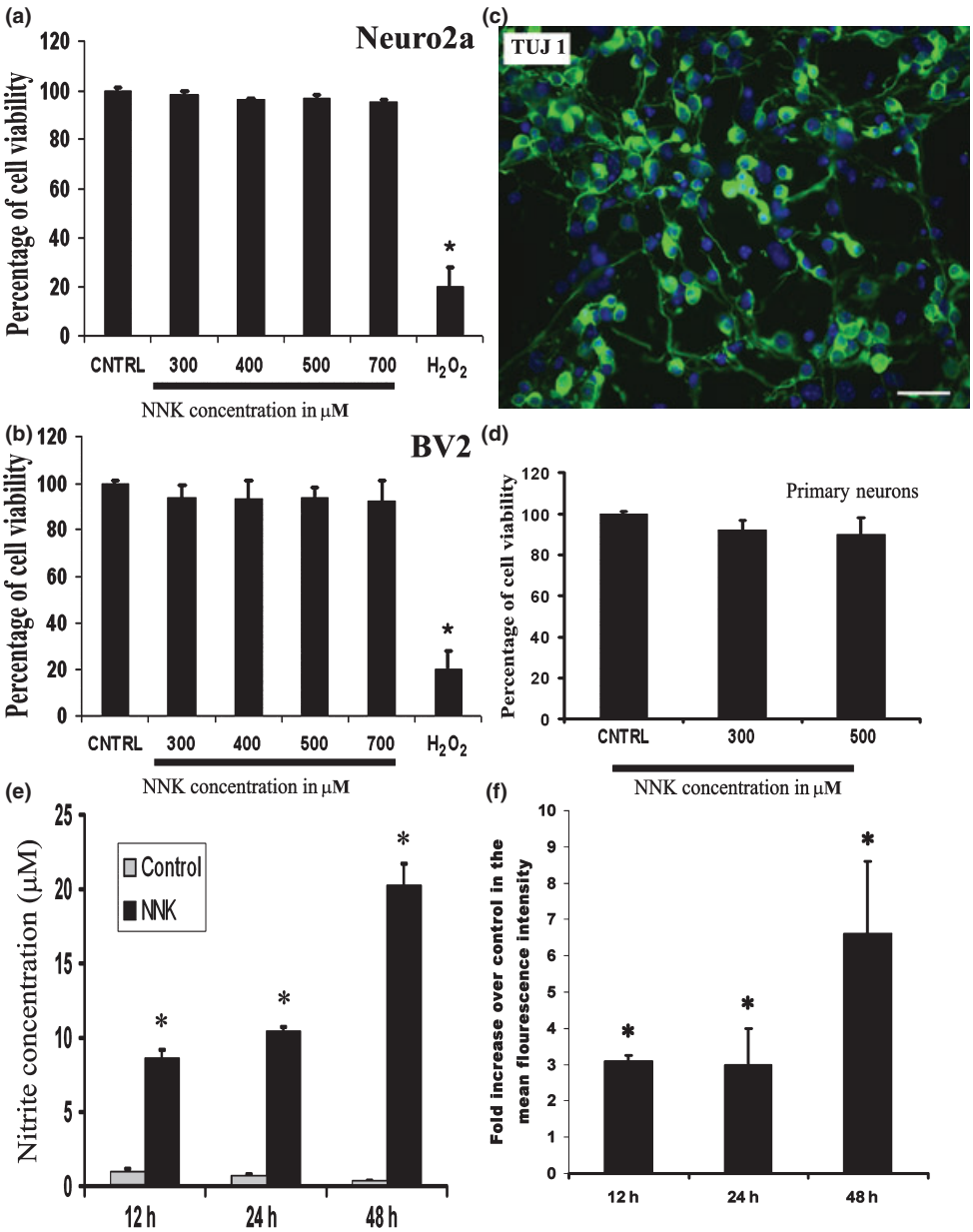

Fig. 1 NNK does not causes direct neuronal or microglial cytotoxicity *in vitro* (a–d). Mouse neuroblastoma Neuro2a cells (N2a) and mouse microglial cells (BV2) were treated with various concentrations of NNK for 48 h. The viability was then evaluated by MTT assay. Figure clearly depicts that NNK does not cause significant direct cellular death to the neuronal and microglial cell lines in a dose even as high as 700 μM (a,b). Primary cortical neurons were cultured from cortices of P2 pups and grown in neurobasal media. Cells were plated at a density of 5×10^3 cells/cm^2 onto poly-D-lysine-coated 96-well plate (Nunc, Roskilde, Denmark). MTT assay was performed after treating the cells with various concentrations of NNK for 48 h. Figure clearly depicts that NNK does not cause significant direct cellular death to the primary neuron in a dose even as high as 500 μM (d). Primary neurons cultured from cortices of the pups were also plated in Labtek chamber were fixed in 4% paraformaldehyde for 20 min, and then stained for primary neuronal marker Beta III Tubulin (c). The Figure is of 20× magnification and scale bar is 25 μm. Asterisks (*) indicate significant difference from the control group ($p < 0.001$; One-way model 1 ANOVA). Data represent mean ± SD from three independent experiments performed in duplicate. NNK induces significant nitric oxide release and intracellular ROS generation in BV2 cells (e,f): BV2 cells were treated with NNK for different time span. Then the cell supernatants of the control and treated cells were collected and assayed for released NO by Griess reagent. The whole-cell lysate of the control and respected treated groups are used for intracellular ROS measurement by DCFDA. (e) NO level in cell supernatant of control and different treatment groups. (f) Fold increase in intracellular ROS level over control in different groups. Asterisks (*) indicate significant difference from the control group ($p < 0.001$; One-way model 1 ANOVA). Data represent mean ± SD from three independent experiments performed in duplicate.

did not cause significant direct cellular death to the neuronal and microglial cell lines in a dose even as high as 700 μM (Fig. 1a and b). Further, we wanted to assess whether NNK is toxic if tested on primary neuronal cells. We cultured primary neuronal cells and performed MTT after treating the cells with different NNK doses. NNK did not cause significant death to primary neurons (Fig. 1d), showing that NNK was not directly toxic to primary neuronal cells.

NNK induces nitric oxide release and intracellular ROS generation in BV2 cells

BV2 cells were treated with 500 μM of NNK for various time points: 12, 24, and 48 h. The whole-cell lysate of the control and NNK-treated groups were used for intracellular ROS measurement by 5- and 6-chloromethyl-2′,7′ dichlorodihydrofluorescein diacetate acetyl ester. Prior to lysis, cells were treated with 5- and 6-chloromethyl-2′,7′ dichlorodihydrofluorescein diacetate acetyl ester (5 mM) for 1 h at 25°C, and then washed twice with 1× phosphate-buffered saline (PBS). The protein obtained was used to measure relative fluorescence by Varioskan Flash Multimode Reader. The cell supernatants of the control and treated cells were collected and assayed for released NO by Griess reagent. Both NO and ROS levels increased gradually with increase in time period of NNK treatment (Fig. 1e and f). Maximum ROS generation and NO release were observed at 48 h of NNK treatment ($p < 0.001$). Data represent mean ± SD from three independent experiments performed in duplicate.

NNK causes up-regulation of inflammation-associated proteins in BV2 cells

Western blot analysis demonstrated a significant induction in the expression of different inflammatory proteins in BV2 cells following NNK treatment (Fig. 2a and b). BV2 cells were treated with NNK of 500 μM concentration for three time points: 12, 24, and 48 h. The whole-cell lysate was used for western blot analysis of the proteins. There was a significant increase in the expression of COX-2, iNOS, phospho-ERK1/2, phospho-p38 MAPK, phospho-JNK, HSP70 ($p < 0.001$), and TRX1 ($p < 0.05$). But phospho-NFκβ, NFκβ, and SOD-1 did not increase significantly. A significant decrease in the expression of IκBα ($p < 0.05$) in the 48 h NNK-treated group when compared with control was observed. Data represent mean ± SD from three independent experiments performed in duplicate. This result showed that MAPK signaling pathway of BV2 could be activated by NNK (Lee *et al.* 2000).

NNK causes up-regulation of proinflammatory cytochemokines in BV2 cells

The up-regulated status of the signaling molecules of microglia activation prompted us to check the proinflamma-

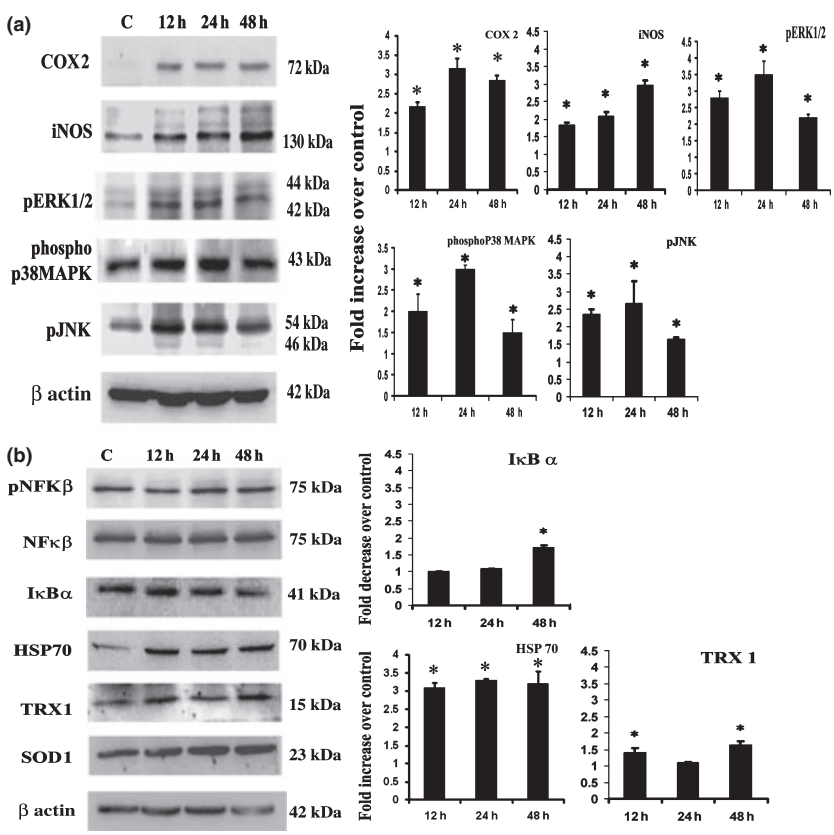

Fig. 2 NNK treatment causes activation of inflammation-associated proteins and stress-induced proteins *in vitro*. Immunoblot analysis of the whole-cell lysate of BV2 cells from control and NNK-treated groups showed a significant increase in the levels of COX-2, iNOS, pERK1/2, phospho-p38MAPK, and pJNK (a) in the NNK-treated cells over control. NNK treatment was carried out for three time points: 12, 24, and 48 h. Figure also shows that there is no significant change in the expression of pNFκβ, NFκβ, and SOD1 at any of the time points of NNK treatment (b). The densitometric analyses of immunoblots are presented as graphs, depicting fold increase in the expression of corresponding proteins over control after different time points of NNK treatment. The expression of HSP70, TRX1, and IκBα shows substantial change at different points of NNK treatment (b). Asterisks (*) indicate significant difference from the control group ($p < 0.001$; One-way model 1 ANOVA); and for TRX1 and IκBα, $p < 0.05$ (One-way model 1 ANOVA). Data represent mean ± SD from three independent experiments performed in duplicate.

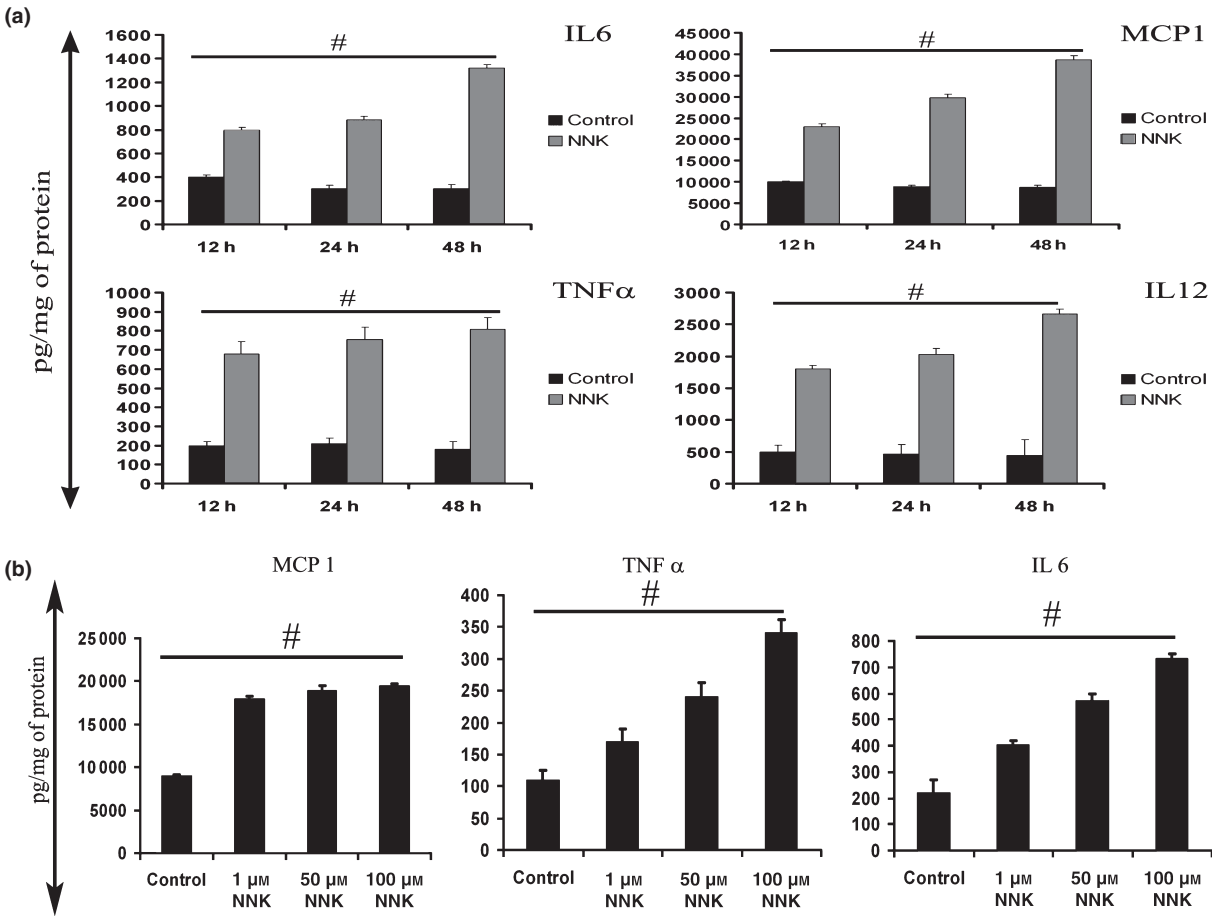

Fig. 3 (a) NNK induces up-regulation of proinflammatory cytochemokines *in vitro*. The figure shows absolute values of proinflammatory cytokines in the whole-cell lysate of BV2 cells after NNK treatment of 12, 24, and 48 h. The whole-cell lysate of control and treated cells of all time point of treatments was analyzed by CBA which showed that treatment with NNK caused significant increase in the expression of proinflammatory mediators like TNF-α, monocyte chemoattractant protein 1 (MCP1), IL-6, and IL-12. For all the cases the proinflammatory cytokine level increased gradually with time of treatment. Asterisks (*) indicate significant difference from the control group ($p < 0.001$; One-way model 1 ANOVA). Data represent mean ± SD from three independent experiments performed in duplicate. (b) NNK induces up-regulation of proinflammatory cytochemokines *in vitro* in a dose-dependent manner. NNK caused significant increase in the expression of proinflammatory mediators like MCP1, TNF-α, and IL-6. The figure shows absolute values of proinflammatory cytokines in the whole-cell lysate of BV2 cells undergoing 24-h treatment of NNK in different doses. For all the cases the proinflammatory cytokine level increased gradually with doses of treatment. # indicate significant difference from the control group ($p < 0.001$; One-way model 1 ANOVA). Data represent mean ± SD from three independent experiments performed in duplicate.

tory cytokine levels in the BV2 cells. BV2 cells were treated with 500 μM of NNK for various time points: 12, 24, and 48 h. CBA analysis showed NNK caused significant increase in the expression of proinflammatory mediators like tumor necrosis factor (TNF)-α, monocyte chemoattractant protein 1 (MCP1), interleukin (IL)-6, and IL-12 (Fig. 3a) in BV2 cells. For all the cases the proinflammatory cytokine level increased gradually with time of NNK treatment.

Again we performed CBA with BV2 cell lysate on a single time point (24 h) treatment with various doses of NNK, starting from a dose as low as 1 μM. Result showed that treatment of BV2 cell with such a low dose also caused significantly high release of proinflammatory cytokines compared with control (Fig. 3b). The cytokine level gradually increased with higher doses.

Data represent mean ± SD from three independent experiments performed in duplicate ($p < 0.001$). This result indicates that NNK causes activation of microglia via MAPK pathway, leading to secretion of inflammatory cytokines.

NNK causes up-regulation of inflammation-associated proteins in mice brain

We then proceeded to explore whether NNK could cause microglial activation *in vivo*. Adult BALB/c mice of either sex were randomly assigned to three groups: (i) control

group receiving PBS (C); (ii) group being administered 10 mg/kg body weight of NNK; and (iii) group being administered 15 mg/kg body weight of NNK. NNK was administered twice daily, i.m. and i.p., in an alternate manner. Treatment of NNK was carried out for 4 days. Western blot analysis of the whole-brain lysate of the control and treated group demonstrated a significant induction in the expression of different inflammatory proteins following NNK treatment (Fig. 4a and b). There was a significant increase in the expression of COX-2, iNOS, phospho-ERK1/2 ($p < 0.05$), phospho-p38 MAPK, phospho-JNK, phospho-NFκβ HSP70, SOD-1, and TRX1.

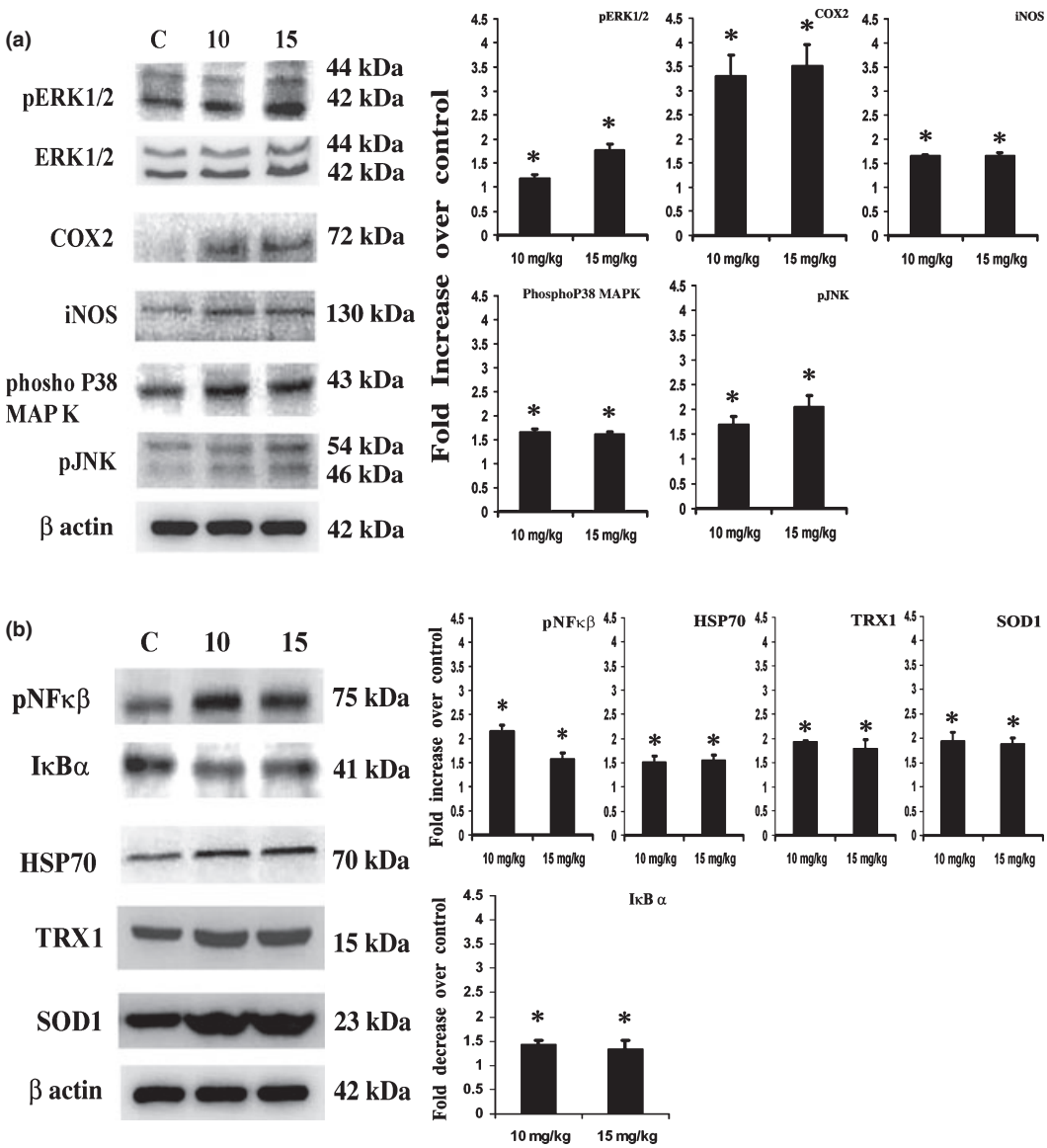

Fig. 4 NNK treatment for 4 days causes activation of inflammation-associated proteins and stress-induced proteins *in vivo*. Adult BALB/c mice of either sex were randomly assigned to three groups: (i) control group (C) being administered PBS; (ii) group being administered 10 mg/kg body weight of NNK; (iii) group being administered 15 mg/kg body weight of NNK. NNK was administered twice daily via i.m. and i.p. route in an alternate manner for 4 days. Immunoblot analysis of the whole-brain lysate of control and treated mice (of both 10 and 15 mg/kg body weight) showed that there was a significant increase in the levels of COX-2, iNOS, pERK1/2, phospho-p38MAPK, and pJNK in the NNK-treated cells over control (a). Again there was significant increase in the expression of pNFκβ, HSP70, TRX1, and SOD1 because of NNK treatment (b). The expression of IκBα shows substantial down-regulation caused by NNK treatment (b). The densitometric analyses of immunoblots are presented as graphs, depicting fold increase in the expression of corresponding proteins over control at different doses of NNK treatment. Asterisks (*) indicate significant difference from the control group ($p < 0.001$; One-way model 1 ANOVA). Data represent mean ± SD from six animals of each group.

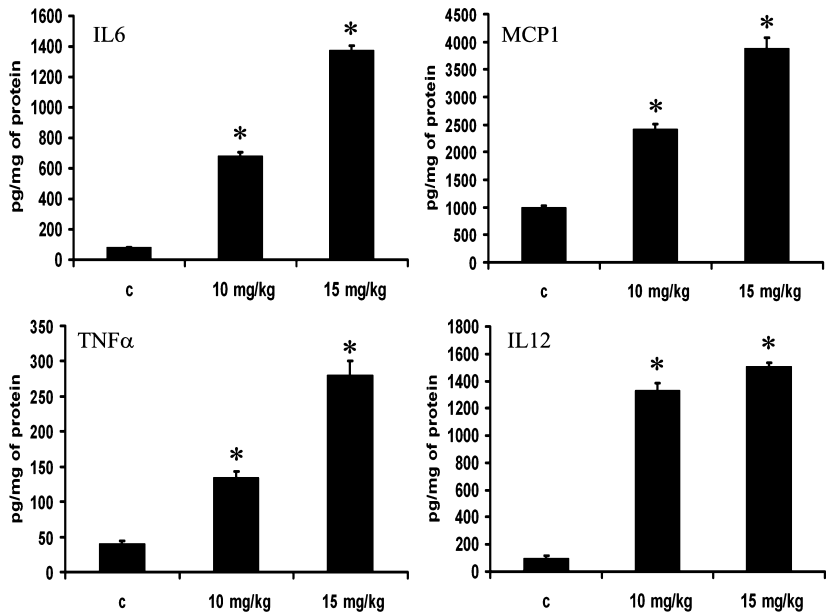

Fig. 5 NNK induces up-regulation of pro-inflammatory cytochemokines in adult mice brain. The whole-brain lysate of control and treated mice (of both 10 and 15 mg/kg body weight) was analyzed by CBA. The figure shows absolute values of proinflammatory cytokines in the whole-brain lysate of mice undergoing 4-day NNK treatment. Treatment with NNK caused significant increase in the expression of proinflammatory mediators like TNF-α, monocyte chemoattractant protein 1 (MCP1), IL-6, and IL-12. The change was more profound in the group treated with 15 mg/kg body weight dose of NNK. Asterisks (*) indicate significant difference from the control group ($p < 0.001$; One-way model 1 ANOVA). Data represent mean ± SD of six animals from each group.

There was also a significant decrease in the expression of IκBα in the NNK-treated group when compared with control. The findings from *in vivo* experiment corresponded to *in vitro* results but increase in phospho-NFκβ level and decrease in IκBα should be taken into account which indicates availability of free NFκβ. Thus, in addition to MAPK pathway the *in vivo* data actually indicate that NFκβ may also play some role ($p < 0.001$). Data represent mean ± SD from six animals of each group.

NNK causes up-regulation of proinflammatory cytokines in mice brain

The cytokine profile of whole-brain lysate of control and 4 day NNK-treated mice (of both 10 and 15 mg/kg body weight) was analyzed by CBA. NNK caused significant increase in the expression of proinflammatory mediators like TNF-α, MCP1, IL-6, and IL-12 (Fig. 5) ($p < 0.001$). Data represent mean ± SD of six animals from each group.

NNK maintains elevated expression of inflammation-associated proteins in mice brain after 12 days of treatment

We next analyzed whether NNK-induced inflammatory condition sustained over considerable time span. The treatment regime of the animals was extended upto 12 days. Western blot analysis of whole-brain lysate for iNOS, phospho-ERK1/2, COX-2, phospho-JNK, phospho-p38 MAPK, phospho-NFκβ, SOD-1, HSP70, and TRX1, demonstrated a significant increase in expression of all the proteins (except SOD-1) following NNK treatment (Fig. 6). The result is quite similar to that of 4 days treatment condition, which depicts that the signaling pathway of microglial activation is still active at 12 days of treatment. ($p < 0.001$). Data represent mean ± SD from six animals of each group.

NNK treatment causes activation of microglia and astrocytes in mice brain

As recent data have suggested that both microglia (Gonzalez-Scarano and Baltuch 1999) and astrocytes (Moynagh 2005) play a major role in brain inflammatory upheaval, we proceeded to check the morphological features of microglial and astroglial population of the control and NNK-treated brain. Cryostat sections of brain from control and NNK-treated mice (15 mg/kg body weight; both 4 and 12 days treatment) were analyzed immunohistochemically for Iba-1, a marker for microglia (Ito *et al.* 2001) and GFAP, a marker for astrocytes. Expression of both Iba-1 and GFAP showed a prominent increase. Substantial microgliosis and astrogliosis (Fig. 7e and b) was noted on day 4 of treatment with robust changes in the morphology of both microglia and astrocytes. On the day 12, although astrogliosis persisted, there was reduced population of activated microglia (Fig. 7c and f). The figures represent cryosections of a mouse brain from each group as a representative of six animals from each group.

We also checked whether NNK activated microglia at a low dose. We performed immunostaining for Iba-1 in mice brains treated with 5 and 0.5 mg/kg doses of NNK. Microglia was moderately activated by 4-day time point when administered a dose of 0.5 mg NNK/kg body weight but we found distinct microglial activation on 12-day-treated mice model. However, microglia activation occurred at 4-day time point when NNK was administered at a dose of 5 mg/kg body weight. Thus, we can predict that lower doses of NNK activate microglial cell, over a longer time span (Fig. S1).

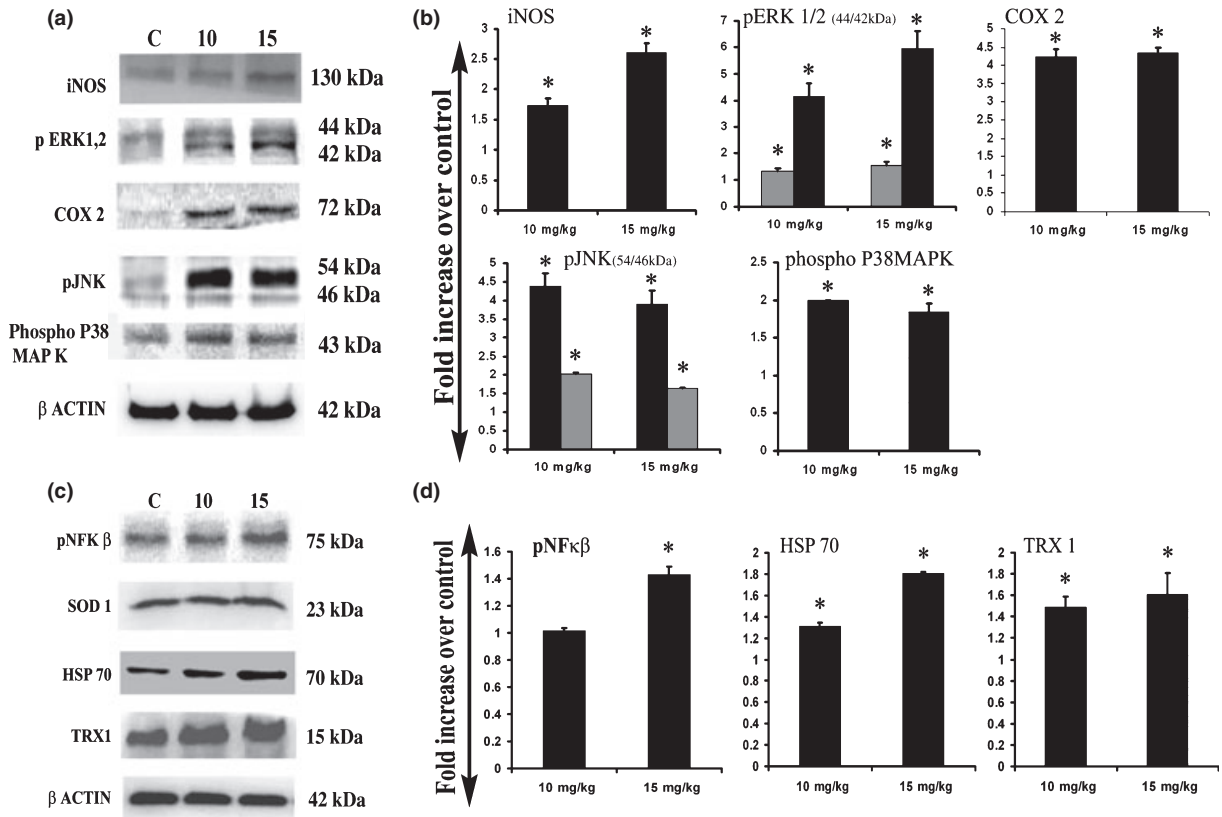

Fig. 6 NNK treatment for 12 days sustains the activation profile of inflammation-associated proteins and stress-induced proteins *in vivo.* NNK treatment was carried out for 12 days at two doses – 10 and 15 mg/kg of body weight, and immunoblot analysis of the whole-brain lysate was performed. Figure shows that there is a significant increase in the levels of iNOS, pERK1/2, COX-2, pJNK, phospho-p38MAPK (a, b), pNFκβ, HSP70, and TRX1 (c, d) expression after NNK treatment. Expression of SOD1, however, showed no significant change from control (b). The densitometric analyses of immunoblots are presented as graphs, depicting fold increase in the expression of corresponding proteins over control at different doses of NNK treatment. Asterisks (*) indicate significant difference from the control group ($p < 0.001$; One-way model 1 ANOVA). Data represent mean ± SD from six animals of each group.

For both higher and lower doses of NNK treatment, astrogliosis and microgliosis were found in cortex of all the regions of brain. But microgliosis was more acute in the cortex over the hippocampus. We have not studied the phenomena in cerebellum or brain stem regions, the investigation of which could be conducted in a separate study.

NNK causes acute neuronal damage in mice brain

Experiments so far have suggested that NNK may cause acute microglial and astroglial activation with profound increase in proinflammatory cytokines and neurotoxic elements. It is obvious that such an environment may trigger neuronal damage and thus we checked the status of the cortical neurons of the control and treated mice. Cryostat sections of brain from control and NNK-treated mice (15 mg/kg; both 4 and 12 days treatment) were analyzed immunohistochemically for NeuN. Substantial neuronal damage was evident from both the 4- and 12-day NNK treatment group when compared with control sections (Fig. 8d–f; Fig. S2). Cryostat sections of brain from control and NNK-treated mice were also processed for thionin and FJC staining. Thionin staining showed distinct change in neuronal morphology in both day 4 and day 12 of treatment groups compared with control (Fig. 8a–c); foci of neurodegeneration was evident in both 4- and 12-day NNK-treated brain sections as observed by FJC staining (Fig. 8g–i). The figures represent cryosections of a mouse brain from each group as a representative of six animals from each group.

We observed by FJC staining that neuronal damage correlated with the microglial actvation. In the lower dose of NNK treatment (0.5 mg/kg), microglia was moderately activated at 4 days but we did not find any foci of neuronal damage by FJC staining (Fig. S3). Again when administered at 5 mg/kg body weight, substantial microglial activation was observed at 4-day time point but we still observed that there were no foci of neurodegeneration. At 12 days of treatment both 0.5 and 5 mg/kg doses resulted in significant

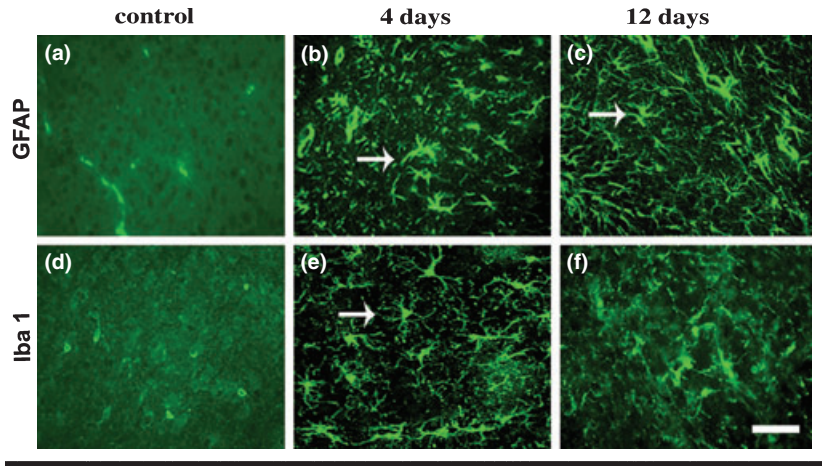

Fig. 7 NNK treatment causes acute microgliosis and astrogliosis activation *in vivo*. Mice were treated with 15 mg/kg body weight of NNK for 4 and 12 days. Then cryostat sections of brain from control (a, d) and treated mice were stained immunohistochemically with Iba-1, a marker for microglia and GFAP, marker for astrocyte. Substantial microgliosis and astrogliosis were noted on day 4 of treatment where there was robust change in the morphology of both microglia and astrocytes (e and b). On the day 12, although astrogliosis persisted (c), there was reduced population of activated microglia (f). The images are of cerebral cortex around the hippocampal region. The figures represent cryosections of a mouse brain of each group as a representative of six animals from each group (40× magnification; Scale Bar: 25 μm).

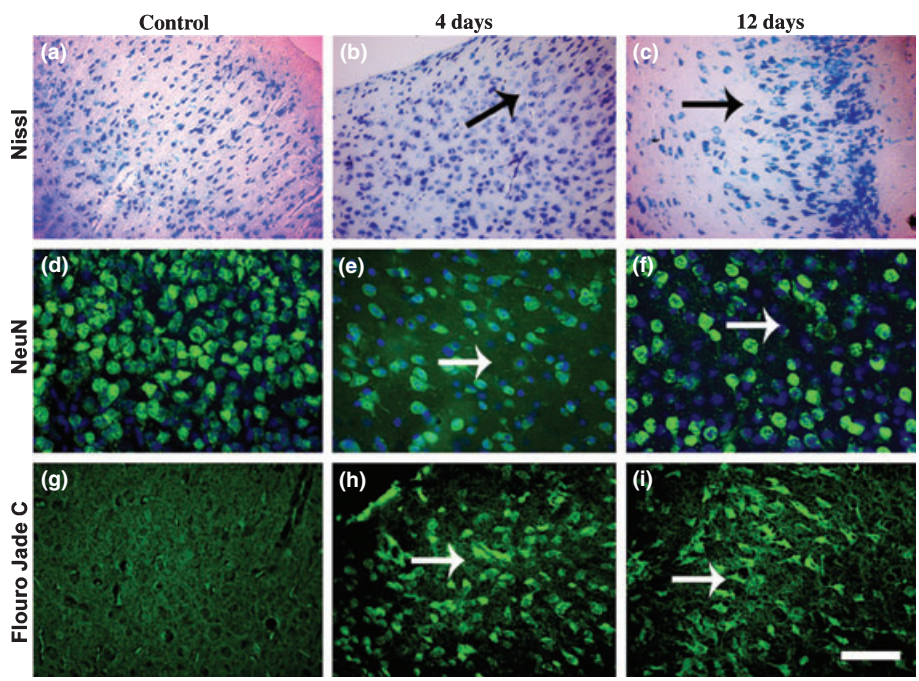

Fig. 8 NNK treatment causes acute neuronal damage *in vivo*. Mice were treated with 15 mg/kg body weight of NNK for 4 and 12 days. Then cryostat sections of brain from control and treated mice of both the treatment groups were stained with the thionin (a–c), NeuN (d,f), and Flouro Jade C (g–i). Thionin staining showed distinct neuronal loss along with morphological alteration in the 4- and 12-day treatment groups respectively. Substantial neuronal loss in both the treatment groups was evident by NeuN staining, while Flouro Jade C staining showed foci of neurodegeneration. The images are of cerebral cortex around the hippocampal region. Figures represent cryosections of mouse brain from each group as a representative of six animals from the group. (a–c: 20× magnification, Scale Bar: 50 μm; d–i: 40× magnifications; Scale Bar: 25 μm).

microgliosis and neurodegenerative foci. This result indicated that microglia activation was followed by neuronal damage. This clearly indicated that neuronal damage might be caused by activated microglia. The foci of neuronal damage (Fig. 8 and Fig. S3) were found in cortical regions of brain but it was more acute in the cortex over the hippocampal zone.

Discussion

Millions of people all over the world practice tobacco smoking. Till date, research in this area has highlighted the carcinogenic and respiratory hazards of tobacco smoke. But studies are scanty regarding the role of tobacco carcinogen NNK in causing neuroinflammation and neuronal damage in brain. This study is the first of its kind that showed that NNK, one of the most potent carcinogens in tobacco smoke, could cause neuroinflammation in mammalian brain.

In our study, we have focused on the role of NNK in microglial activation because microglia has been the pivotal part of neuroinflammation and several neurodegenerative disorders (Gonzalez-Scarano and Baltuch 1999; Streit *et al.* 2004; Jack *et al.* 2005). Microglia, the primary immune cells of the central nervous system, is particularly sensitive to changes in their microenvironment and readily become activated in response to infection or injury. In a non-regenerating organ such as the brain, a dysregulated innate immune response can be deleterious. Thus, microglia that remain activated for extended periods of time can damage nearby neurons.

The major findings of our study are (i) NNK causes microglial activation *in vitro* and *in vivo*, (ii) NNK induces the elevation of proinflammatory signaling and effector molecules *in vitro* and *in vivo*, and (iii) NNK causes indirect neuronal damage *in vivo*.

4-*N*-methyl-*N*-nitrosamino-1-(3-pyridyl)-1-butanone entered the body through lungs where it was metabolized considerably into its active form by lung enzymes (Akopyan and Bonavida 2006). Alhough there were no data showing that NNK could cross the blood–brain barrier, recent studies have shown NNK to be highly lipid-soluble (Jorquera *et al.* 1992; Gerde *et al.* 1998); Again most of the substrates of CYP2B6 which include NNK are generally small hydrophobic molecules having low-permeability surface area, suggesting that most CYP2B6 substrates are active in CNS and can cross the blood–brain barrier (Liu *et al.* 2004; Ekins *et al.* 2008). CYP2A6, CYP2A13, CYP3A4, CYP3A5, CYP2E1, and CYP2B6 are considered to be P450 enzymes, most likely to be active in the human pulmonary biotransformation of NNK. However, we are not sure whether pulmonary CYP enzymes could metabolize all the NNK absorbed. Some of these CYP enzymes are also widely present in liver and brain (Stevens *et al.* 1997; Higashi *et al.* 2007). Thus, NNK is administered both via i.p. and i.m. route to provide NNK in both metabolized and unmetabolized form to the brain, thereby mimicking the *in vivo* situation as close as possible.

The concentration of NNK in the mainstream cigarette smoke could be as high as 1.749 ng (Fischer *et al.* 1990a,b; Harris 2004). Again it has been shown previously that nicotine can be metabolized in liver into NNK precursor molecule (Hecht *et al.* 2000), moreover the half lives of NNK metabolites are long and they have a slow clearance rate (Hecht *et al.* 1999; Jacob *et al.* 2008). These properties qualifies NNK to be a compound wherein toxicity effect could be estimated by Haber's Law (Saghir *et al.* 2005) which states that concentration × time = constant. Thus, to estimate the effect NNK might have for prolong period of time (few years), we have administered 10 and 15 mg/kg body weight of NNK for most of our *in vivo* experiments for 4 and 12 days. However, we have also shown in the Figs. S2 and S3 that NNK administered at a dose of 0.5 mg/kg leads to substantial activation of microglial and subsequent neuronal damage. Moreover, BV2 cells exposed to NNK at a dose as low as 1 μM can get activated and release inflammatory cytokines. Thus low doses of NNK do activate microglia. Again we have found out that there is a relationship between dose and time period of treatment. Microglia was only slightly activated by 4-day time point when NNK was administered at a dose of 0.5 mg/kg body weight but at a dose of 5 mg/kg, microglia was activated by 4 days. Interestingly, for both the doses there were no neurodegenerative foci at 4 days. After 12 days of treatment both 0.5 and 5 mg/kg doses resulted in significant microgliosis and neurodegenerative foci (Fig. S3). Thus microglia activation was followed by neuronal damage. Again our MTT data (Fig. 1a–d) showed that 500 μM of NNK did not kill N2a or the primary neurons even after 48 h. This clearly indicated that neuronal damage might be caused by activated microglia, and not directly by NNK. Thus we can predict that lower doses of NNK activate microglial cell, over a longer time span, and this chronic activation may be very harmful for neurons. In fact, reports state that prolonged smoking caused cognitive decline among middle-aged men and women (Sabia *et al.* 2008).

The *in vitro* experiments showed that NNK may cause BV2 cells to become activated and secrete proinflammatory cytochemokines. However, NNK treatment of BV2 cells did not cause pNFκβ induction but the decrease of Iκβα was found 48 h after the addition of NNK. At this time point however, pro-inflammatory genes were already up-regulated. So the decrease in Iκβα was not related to the microglia activation as found here but might play a role when NNK was exposed for more than 48 h. Thus NNK may activate microglia by another signaling pathway and detailed studies are needed to fully elucidate the signaling pathway by which NNK activates microglia. Our work shows that microglia are being activated by the MAPK pathway which ultimately induces signaling molecules like pERKs, pJNK, and p38MAPK while triggering transcription of COX-2. NNK treatment also leads to the production of neurotoxic mediators like TNF-α. In our *in vitro* experiments found that in most cases the proinflammatory proteins was increased to maximum, much before ROS generation reached its maximum. Thus, further studies are needed to clarify the sequence of events that lead to the microglial activation. In our *in vivo*

model, immunoblot analysis showed higher expression of pNFκβ along with pERKs, pJNK, and p38MAPK in the NNK-treated brains. The increase in pNFκβ in this case might be because of the activated astrocytes which were present in vast numbers in the brain. The literature shows that inflammatory cytokines from microglia activate astrocytes (Moynagh 2005) via signaling pathways involving NFκβ but we cannot rule out the fact that NNK may activate astrocytes directly.

In Fig. 7 and Fig. S1, the Iba-1 staining of the mice treated for 4 days shows robust microglial activation. This finding is reinforced by increased expression of microglial signaling molecules like pERKs, pJNK, and p38MAPK. The CBA analysis shows dramatic increase in proinflammatory cytochemokine levels in the brain; and all this evidence suggests that the neuronal damage is caused by the activated microglia and astrocytes. However, fewer activated microglia were observed at 12 days when administered higher doses of NNK (Fig. 7) but astrocyte activation was still robust. The inflammatory mediators secreted by microglia may provide a negative feedback to the microglia causing them to return to the inactive state. This hypothesis is supported by the fact that we did not detect any significant levels of proinflammatory cytochemokines on day 12 brain samples. It is very interesting that in high dose of 15 mg/kg body weight, 12 days treatment with NNK caused microglia to become quiescent or less activated but in lower dose of 0.5 and 5 mg/kg microglia was more activated with prolonged NNK treatment (Fig. S1). Thus NNK in low dose taken for prolong period may cause chronic microglial activation and this inflamed milieu may be extremely harmful for neurons.

TRX1 and SOD1 play a protective role against the ROS (Halliwell 1992; Gabai *et al.* 1997). In 4-day NNK-treated brain, increased levels of both the proteins were observed. This up-regulation of SOD1 and TRX1 may be intrinsic response of body against the generated oxidative stress. Interestingly, after 12 days of NNK treatment the SOD1 expression was decreased to normal. Thus NNK may inhibit SOD1 expression in longer time period, thus amplifying the oxidative stress.

In conclusion, we can state that NNK can induce acute inflammation in brain leading to neuronal damage and can aggravate conditions in neuroinflammation-mediated pathological conditions. We also highlighted in this study that NNK in a low concentration activated microglia over a longer time period.

Acknowledgements

This work was supported by grant awarded to AB from the Department of Biotechnology (DBT). This work is also supported by a core grant from DBT to NBRC. MKM and SD are a recipient of Senior Research Fellowship from University Grants Commission. DKK is a recipient of Junior Research Fellowship from Indian Council of Medical Research.

We thank Parthiv Haldipur, Kanhaiya Lal Kumawat, and Manish Dogra for their assistance in this work. We deeply acknowledge Dr Ramdas Chatterjee from Chittaranjan National Cancer Institute, Calcutta, for his encouragement in this study. We thank Prof. Vijayalakshmi Ravindranath, Director NBRC, for her continuous interest in our research program.

Supporting Information

Additional Supporting Information may be found in the online version of this article:

Figure S1. NNK treatment causes acute microgliosis *in vivo* even at lower doses.

Figure S2. Graphical representation of the quantification of the neuronal loss (observed by NeuN staining) in 15 mg/kg body weight NNK-treated mice brain in compared with control.

Figure S3. NNK treatment causes neuronal damage *in vivo* even at lower dose.

Appendix S1. Supplementary Materials and methods.

As a service to our authors and readers, this journal provides supporting information supplied by the authors. Such materials are peer-reviewed and may be re-organized for online delivery, but are not copy-edited or typeset. Technical support issues arising from supporting information (other than missing files) should be addressed to the authors.

References

Akopyan G. and Bonavida B. (2006) Understanding tobacco smoke carcinogen NNK and lung tumorigenesis. *Int. J. Oncol.* **29**, 745–752.

Basu A., Krady J. K., O'Malley M., Styren S. D., DeKosky S. T. and Levison S. W. (2002) The type 1 interleukin-1 receptor is essential for the efficient activation of microglia and the induction of multiple proinflammatory mediators in response to brain injury. *J. Neurosci.* **22**, 6071–6082.

Basu A., Lazovic J., Krady J. K., Mauger D. T., Rothstein R. P., Smith M. B. and Levison S. W. (2005) Interleukin-1 and the interleukin-1 type 1 receptor are essential for the progressive neurodegeneration that ensues subsequent to a mild hypoxic/ischemic injury. *J. Cereb. Blood Flow Metab.* **25**, 17–29.

Bhagwat S. V., Vijayasarathy C., Raza H., Mullick J. and Avadhani N. G. (1998) Preferential effects of nicotine and 4-(*N*-methyl-*N*-nitrosamine)-1-(3-pyridyl)-1-butanone on mitochondrial glutathione *S*-transferase A4-4 induction and increased oxidative stress in the rat brain. *Biochem. Pharmacol.* **56**, 831–839.

Ekins S., Iyer M., Krasowski M. D. and Kharasch E. D. (2008) Molecular characterization of CYP2B6 substrates. *Curr. Drug Metab.* **9**, 363–373.

Fischer S., Castonguay A., Kaiserman M., Spiegelhalder B. and Preussmann R. (1990a) Tobacco-specific nitrosamines in Canadian cigarettes. *J. Cancer Res. Clin. Oncol.* **116**, 563–568.

Fischer S., Spiegelhalder B. and Preussmann R. (1990b) Tobacco-specific nitrosamines in European and USA cigarettes. *Arch. Geschwulstforsch* **60**, 169–177.

Gabai V. L., Meriin A. B., Mosser D. D., Caron A. W., Rits S., Shifrin V. I. and Sherman M. Y. (1997) Hsp70 prevents activation of stress

kinases. A novel pathway of cellular thermotolerance. *J. Biol. Chem.* **272**, 18033–18037.

Gao W. O., Heintz N. and Hatten M. E. (1991) Cerebellar granule cell neurogenesis is regulated by cell-cell interactions in vitro. *Neuron* **6**, 705–715.

Gerde P., Muggenburg B. A., Stephens T., Lewis J. L., Pyon K. H. and Dahl A. R. (1998) A relevant dose of 4-(methylnitrosamino)-1-(3-pyridyl)-1-butanone is extensively metabolized and rapidly absorbed in the canine tracheal mucosa. *Cancer Res.* **58**, 1417–1422.

Ghoshal A., Das S., Ghosh S., Mishra M. K., Sharma V., Koli P., Sen E. and Basu A. (2007) Proinflammatory mediators released by activated microglia induces neuronal death in Japanese encephalitis. *Glia* **55**, 483–496.

Gonzalez-Scarano F. and Baltuch G. (1999) Microglia as mediators of inflammatory and degenerative diseases. *Annu. Rev. Neurosci.* **22**, 219–240.

Griffin W. S. (2006) Inflammation and neurodegenerative diseases. *Am. J. Clin. Nutr.* **83**, 470S–474S.

Halliwell B. (1992) Reactive oxygen species and the central nervous system. *J. Neurochem.* **59**, 1609–1623.

Harris J. E. (2004) Incomplete compensation does not imply reduced harm: yields of 40 smoke toxicants per milligram nicotine in regular filter versus low-tar cigarettes in the 1999 Massachusetts Benchmark Study. *Nicotine Tob. Res.* **6**, 797–807.

Hecht S. S., Carmella S. G., Chen M., Dor Koch J. F., Miller A. T., Murphy S. E., Jensen J. A., Zimmerman C. L. and Hatsukami D. K. (1999) Quantitation of urinary metabolites of a tobacco-specific lung carcinogen after smoking cessation. *Cancer Res.* **59**, 590–596.

Hecht S. S., Hochalter J. B., Villalta P. W. and Murphy S. E. (2000) 2′-Hydroxylation of nicotine by cytochrome P450 2A6 and human liver microsomes: formation of a lung carcinogen precursor. *Proc. Natl Acad. Sci. USA* **97**, 12493–12497.

Hellermann G. R., Nagy S. B., Kong X., Lockey R. F. and Mohapatra S. S. (2002) Mechanism of cigarette smoke condensate-induced acute inflammatory response in human bronchial epithelial cells. *Respir. Res.* **3**, 22.

Higashi E., Nakajima M., Katoh M., Tokudome S. and Yokoi T. (2007) Inhibitory effects of neurotransmitters and steroids on human CYP2A6. *Drug Metab. Dispos.* **35**, 508–514.

Ito D., Tanaka K., Suzuki S., Dembo T. and Fukuuchi Y. (2001) Enhanced expression of Iba1, ionized calcium-binding adapter molecule 1, after transient focal cerebral ischemia in rat brain. *Stroke* **32**, 1208–1215.

Jack C., Ruffini F., Bar-Or A. and Antel J. P. (2005) Microglia and multiple sclerosis. *J. Neurosci. Res.* **81**, 363–373.

Jacob P. III, Havel C., Lee D. H., Yu L., Eisner M. D. and Benowitz N. L. (2008) Subpicogram per milliliter determination of the tobacco-specific carcinogen metabolite 4-(methylnitrosamino)-1-(3-pyridyl)-1-butanol in human urine using liquid chromatography-tandem mass spectrometry. *Anal. Chem.* **80**, 8115–8121.

Jin Z., Gao F., Flagg T. and Deng X. (2004) Tobacco-specific nitrosamine 4-(methylnitrosamino)-1-(3-pyridyl)-1-butanone promotes functional cooperation of Bcl2 and c-Myc through phosphorylation in regulating cell survival and proliferation. *J. Biol. Chem.* **279**, 40209–40219.

Jorquera R., Castonguay A. and Schuller H. M. (1992) Placental transfer of 4-(methylnitrosamino)-1-(3-pyridyl)-1-butanone instilled intratracheally in Syrian golden hamsters. *Cancer Res.* **52**, 3273–3280.

Lee Y. B., Schrader J. W. and Kim S. U. (2000) p38 map kinase regulates TNF-alpha production in human astrocytes and microglia by multiple mechanisms. *Cytokine* **12**, 874–880.

Liu X., Tu M., Kelly R. S., Chen C. and Smith B. J. (2004) Development of a computational approach to predict blood–brain barrier permeability. *Drug Metab. Dispos.* **32**, 132–139.

Menzin J., Lang K., Friedman M., Neumann P. and Cummings J. L. (1999) The economic cost of Alzheimer's disease and related dementias to the California Medicaid program (''Medi-Cal'') in 1995. *Am. J. Geriatr. Psychiatry* **7**, 300–308.

Mishra M. K., Koli P., Bhowmick S. and Basu A. (2007) Neuroprotection conferred by astrocytes is insufficient to protect animals from succumbing to Japanese encephalitis. *Neurochem. Int.* **50**, 764–773.

Mookerjee Basu J., Mookerjee A., Sen P. *et al.* (2006) Sodium antimony gluconate induces generation of reactive oxygen species and nitric oxide via phosphoinositide 3-kinase and mitogen-activated protein kinase activation in *Leishmania donovani*-infected macrophages. *Antimicrob. Agents Chemother.* **50**, 1788–1797.

Moynagh P. N. (2005) The interleukin-1 signalling pathway in astrocytes: a key contributor to inflammation in the brain. *J. Anat.* **207**, 265–269.

Nakayama T., Kaneko M., Kodama M. and Nagata C. (1985) Cigarette smoke induces DNA single-strand breaks in human cells. *Nature* **314**, 462–464.

Proulx L. I., Gaudreault M., Turmel V., Augusto L. A., Castonguay A. and Bissonnette E. Y. (2005) 4-(Methylnitrosamino)-1-(3-pyridyl)-1-butanone, a component of tobacco smoke, modulates mediator release from human bronchial and alveolar epithelial cells. *Clin. Exp. Immunol.* **140**, 46–53.

Sabia S., Marmot M., Dufouil C. and Singh-Manoux A. (2008) Smoking history and cognitive function in middle age from the Whitehall II study. *Arch. Intern. Med.* **168**, 1165–1173.

Saghir S. A., Lebofsky M., Pinson D. M. and Rozman K. K. (2005) Validation of Haber's Rule (dose × time = constant) in rats and mice for monochloroacetic acid and 2,3,7,8-tetrachlorodibenzo-*p*-dioxin under conditions of kinetic steady state. *Toxicology* **215**, 48–56.

Schmued L. C., Stowers C. C., Scallet A. C. and Xu L. (2005) Fluoro-Jade C results in ultra high resolution and contrast labeling of degenerating neurons. *Brain Res.* **1035**, 24–31.

Stevens J. C., White R. B., Hsu S. H. and Martinet M. (1997) Human liver CYP2B6-catalyzed hydroxylation of RP 73401. *J. Pharmacol. Exp. Ther.* **282**, 1389–1395.

Streit W. J., Mrak R. E. and Griffin W. S. (2004) Microglia and neuroinflammation: a pathological perspective. *J. Neuroinflammation* **1**, 14.

Swarup V., Ghosh J., Ghosh S., Saxena A. and Basu A. (2007) Antiviral and anti-inflammatory effects of rosmarinic acid in an experimental murine model of Japanese encephalitis. *Antimicrob. Agents Chemother.* **51**, 3367–3370.

Swarup V., Ghosh J., Das S. and Basu A. (2008) Tumor necrosis factor receptor-associated death domain mediated neuronal death contributes to the glial activation and subsequent neuroinflammation in Japanese encephalitis. *Neurochem. Int.* **52**, 1310–1321.

Weng M. W., Hsiao Y. M., Chen C. J., Wang J. P., Chen W. C. and Ko J. L. (2004) Benzo[a]pyrene diol epoxide up-regulates COX-2 expression through NF-kappaB in rat astrocytes. *Toxicol. Lett.* **151**, 345–355.

